Polymer Bianchi-I with polymer matter

Aleena Zulfiqar*

Department of Mathematics, Syed Babar Ali School of Science and Engineering, Lahore University of Management Sciences, Lahore 54792, Pakistan

Syed Moeez Hassan[†]

Department of Physics, Syed Babar Ali School of Science and Engineering, Lahore University of Management Sciences, Lahore 54792, Pakistan (Dated: September 30, 2025)

We analyze the effective dynamics of a polymer quantized homogeneous and anisotropic Bianchi-I universe coupled to a polymer quantized scalar field. We use a pressureless dust field as an internal clock, and work with the gravitational Misner variables. We find that for a consistent polymer quantization of the anisotropies, the volume variable has to be polymerized first, and that a choice of different polymer scales for the two leads to substantially different dynamics. We derive an effective Friedmann equation for this model, and also compute the shear scalar. We show that polymer quantizing the scalar field leads to significant differences in the evolution of various cosmological quantities as compared to standard quantization. Furthermore, there is asymmetric evolution across the bounce for both the volume variable and the anisotropies. The amount of these variations and asymmetry, as well as the location of the quantum bounce, depends on the matter polymer scale.

I. INTRODUCTION

One of the major open quests of modern physics is to gain insight into the quantum nature of spacetime. Using a background independent quantization scheme, Loop Quantum Gravity (LQG), and its cosmological manifestation Loop Quantum Cosmology (LQC), have yielded important results, including for example, a resolution of the initial big-bang singularity [1–3]. A method of quantization motivated from loop quantization is that of polymer quantization which introduces a fundamental discreteness in the theory [4, 5]. Polymer quantization has been applied to both gravi-

^{*} aleena.706@lums.edu.pk

[†] syed_hassan@lums.edu.pk

tational models [6–11] (with results similar to those produced by LQC [12]), and to matter systems in order to investigate the effects of such a quantization scheme on matter dynamics [13–22].

Although much of the existing literature has concentrated on homogeneous and isotropic spacetimes [23, 24], it is possible that the early universe (or even the late time universe) passed through anisotropic phases [25–30]. The Bianchi-I model, as the simplest anisotropic cosmological model, serves as a natural framework to investigate such scenarios. Studies within LQC have demonstrated that the effective dynamics of Bianchi-I spacetimes resolve the classical singularity, and that the anisotropies introduce significant modifications to the behavior of the universe in the Planckian regime [31, 32].

From a fundamental perspective, if gravity is in fact polymer quantized, it would be natural to expect that any matter field would also follow the same quantization scheme [33]. Some models of this type have been studied before [34–36], and a first detailed treatment of the effective dynamics of a homogeneous and isotropic Friedmann-Lemaitre-Robertson-Walker (FLRW) universe coupled to a polymer quantized scalar field appeared in [24]. In this study, we extend the model presented in [24] to a homogeneous but anisotropic Bianchi-I spacetime. We polymer quantize the spacetime, and couple it to a polymer quantized massless scalar field. We then study the effective dynamics arising from this model by using a pressureless dust field as an internal clock.

Effective dynamics offer a simpler way of quantifying the main quantum effects of a model without having to resort to the full quantum theory. They are obtained by computing the expectation value of the Hamiltonian in suitable 'semi-classical' states [37, 38]. And although they serve only as a starting point for a complete quantum treatment, they are surprisingly effective [39]. These effective dynamics are then studied with respect to a dust field acting as a clock [40, 41]. A major advantage of choosing dust is that the physical (reduced) Hamiltonian is linear in the Hamiltonians of the remaining degrees of freedom (unlike for example, with scalar field time, or other clock choices [1, 2]). The quantum dynamics arising from using dust as a clock have been investigated in detail for many different gravitational models [42–47].

The remainder of this paper is organized as follows. In Section II, we introduce the model, outline the essentials of polymer quantization, and derive the effective Hamiltonian. The effective Friedmann equation is derived in Section III. In Section IV, we examine the dynamics of this system and present numerical results for both pure gravity and gravity coupled to matter. A summary of

our results and concluding remarks are provided in Section V. Throughout, we employ Planck units with $c = \hbar = 8\pi G = 1$.

II. PHYSICAL HAMILTONIAN AND BIANCHI-1 MODEL

We begin with General Relativity written in the Arnowitt-Deser-Misner (ADM) form, coupled to a massless scalar field ϕ and a pressureless dust field T,

$$S = \int d^3x dt \left[\pi^{ab} \dot{q}_{ab} + p_T \dot{T} + p_\phi \dot{\phi} - N\mathcal{H} - N^a C_a \right], \tag{1}$$

where,

$$\mathcal{H} = \frac{1}{\sqrt{q}} \left(\pi^{ab} \pi_{ab} - \frac{1}{2} \pi^2 \right) - \sqrt{q} R$$

$$+ \frac{p_{\phi}^2}{2\sqrt{q}} + \frac{1}{2} \sqrt{q} q^{ab} \partial_a \phi \partial_b \phi$$

$$+ p_T \sqrt{1 + q^{ab} \partial_a T \partial_b T}, \qquad (2)$$

$$C_a = D_b \pi_a^b + p_\phi \partial_a \phi - p_T \partial_a T, \tag{3}$$

are the Hamiltonian and diffeomorphism constraints respectively. (ϕ, p_{ϕ}) , (T, p_T) and (q_{ab}, π^{ab}) are the scalar field, dust field and gravitational phase space variables respectively, q is the determinant of the spatial metric q_{ab} , π is the trace of π^{ab} , R is the 3-Ricci scalar curvature, N is the lapse and N^a is the shift.

We reduce the full theory to a homogeneous but anisotropic Bianchi-I universe. The line element of this model is,

$$ds^{2} = -dt^{2} + a_{1}^{2}(t)dx^{2} + a_{2}^{2}(t)dy^{2} + a_{3}^{2}(t)dz^{2},$$
(4)

where $a_1(t), a_2(t)$ and $a_3(t)$ are the scale factors corresponding to the three different coordinate directions, and the volume variable is $v = a_1 a_2 a_3$. From these scale factors, we can define directional Hubble parameters H_i as,

$$H_i = \frac{\dot{a}_i}{a_i},\tag{5}$$

with the mean Hubble parameter (H_b) given as,

$$H_b = \frac{1}{3} (H_1 + H_2 + H_3). \tag{6}$$

Another variable of interest (that measures the anisotropy of spacetime) is the shear, which is defined for each direction as the corresponding Hubble parameter minus the mean Hubble parameter, ¹

$$\Sigma_i = H_i - H_b \tag{7}$$

and, the shear scalar,

$$\Sigma^2 = \frac{1}{3} \left(\Sigma_1^2 + \Sigma_2^2 + \Sigma_3^2 \right). \tag{8}$$

In what follows, we work with the more convenient Misner variables defined as,

$$a_1(t) = e^{\alpha} e^{\beta_+ + \sqrt{3}\beta_-}, \qquad a_2(t) = e^{\alpha} e^{\beta_+ - \sqrt{3}\beta_-}, \qquad a_3(t) = e^{\alpha} e^{-2\beta_+},$$
 (9)

and, the line element takes the form,

$$ds^{2} = -dt^{2} + e^{2\alpha}(e^{2\beta})_{ij}dx^{i}dx^{j}, \tag{10}$$

where, α is related to the volume v as $v = e^{3\alpha}$, and β is a traceless diagonal matrix containing the two independent anisotropies β_+ and β_- as $diag(\beta_+ + \sqrt{3}\beta_-)$, $\beta_+ - \sqrt{3}\beta_-$, $-2\beta_+$). With this ansatz, the gravitational phase space variables become,

$$q_{ij} = e^{2\alpha} \left(e^{2\beta} \right)_{ij} ,$$

$$\pi^{ij} = \frac{(p_{+}E_{+}^{ij} + p_{-}E_{-}^{ij} + q^{ij}p_{\alpha})}{2} ,$$
(11)

where $E_{+ij} = diag(1, 1, -2)$, $E_{-ij} = diag(\sqrt{3}, -\sqrt{3}, 0)$, and (p_{α}, p_{\pm}) are the conjugate momenta of (α, β_{\pm}) respectively. We further impose the requirement that both the scalar and dust fields are spatially homogeneous, consistent with the homogeneity of the background universe,

$$(\phi, p_{\phi}, T, p_T) = (\phi(t), p_{\phi}(t), T(t), p_T(t)).$$
 (12)

With this reduction, the diffeomorphism constraint vanishes identically, and the action becomes,

$$S = V_0 \int dt \left(p_{\alpha} \dot{\alpha} + p_{+} \dot{\beta}_{+} + p_{-} \dot{\beta}_{-} + p_{\phi} \dot{\phi} + p_{T} \dot{T} - NH \right), \tag{13}$$

¹ Note that we are using a slightly different notation for the shears (Σ) as compared to the literature (σ), since we use the variable σ for state widths that appear later.

where,

$$H = -\frac{1}{48e^{3\alpha}}(p_{\alpha}^2 - p_{+}^2 - p_{-}^2) + e^{3\alpha}\Lambda + \frac{p_{\phi}^2}{2e^{3\alpha}} + p_T \approx 0$$
 (14)

is the Hamiltonian constraint in Misner variables, and $V_0 = \int d^3x$ is a fiducial volume.

We now choose the dust field as an internal clock, t = -T, and explicitly solve the classical Hamiltonian constraint to obtain a reduced physical Hamiltonian (for further details, we refer to, [40, 41], and we are following the conventions of [20]),

$$H_p = p_T = \frac{1}{48e^{3\alpha}}(p_\alpha^2 - p_+^2 - p_-^2) - e^{3\alpha}\Lambda - \frac{p_\phi^2}{2e^{3\alpha}}.$$
 (15)

Since our goal will be to polymer-quantize this theory, we perform one more canonical transformation (at the classical level) to the volume variable, where the conjugate momentum to the volume is appropriately de-densitized. This is important since polymer quantization involves variables constructed by exponentiating the momenta, and therefore, the momenta must be scalars [17]. The new variables are,

$$v = e^{3\alpha} , \ p_v = \frac{p_\alpha}{3e^{3\alpha}} = \frac{p_\alpha}{3v},$$
 (16)

and the physical Hamiltonian becomes,

$$H_p = H_v - H_+ - H_- - H_\phi, (17)$$

where

$$H_{v} = \frac{3}{16}vp_{v}^{2} - v\Lambda, \quad H_{+} = \frac{p_{+}^{2}}{48v},$$

$$H_{-} = \frac{p_{-}^{2}}{48v}, \quad H_{\phi} = \frac{p_{\phi}^{2}}{2v}.$$
(18)

Our next step is to polymer quantize this Hamiltonian. We first polymer quantize the volume variable (in the next subsection), and then proceed to coupling it to the polymer quantized anisotropies and a polymer quantized scalar field. Note that there is a subtlety involved here that did not occur for the FLRW case [24]: the anisotropy momenta p_{\pm} , just like the scalar field momentum p_{ϕ} , are not scalars, and hence, directly polymer quantizing them is not reasonable. One possible solution is to de-densitize them as well at the classical level by considering a transformation of the form $p_{\pm} \to p_{\pm}/v$. However, this transformation is non-canonical, and produces a Hamiltonian

that is quite complicated. Here, we employ an alternate approach that begins by realizing that the anisotropies behave exactly (mathematically) like a massless scalar field (18). This means that the same method that is used to polymer quantize a scalar field on a given background can be applied to the anisotropies. This is the approach we present here: the volume variable is polymer quantized, and an effective background obtained. Both the anisotropies, and the scalar field, are then polymer quantized on this effective background.²

A. Polymer quantization of Bianchi-I

We start with the polymer quantization of the volume variable (the H_v part of the full Hamiltonian (17)), and take the basic variables to be the volume v, and the exponential of the momentum conjugate to the volume $U \equiv \exp(i\lambda_v p_v)$ which satisfy the Poisson bracket relation,

$$\{v, U\} = i\lambda_v U. \tag{19}$$

Polymer quantization proceeds by promoting these variables to operators on the Hilbert space $L^2(\mathbb{R}_{Bohr})$, where \mathbb{R}_{Bohr} is the Bohr compactification of the real line. A basis for this Hilbert space is provided by the states $|\nu\rangle$ with the inner product,

$$\langle \nu | \nu' \rangle = \delta_{\nu,\nu'},$$
 (20)

where $\delta_{\nu,\nu'}$ is the generalization of the Kronecker delta to real numbers. The action of the basic operators on these states is given as,

$$\widehat{v}|\nu\rangle = \nu|\nu\rangle , \ \widehat{U}|\nu\rangle = |\nu + \lambda_v\rangle,$$
 (21)

with the commutator relation $[\widehat{v}, \widehat{U}] = \lambda_v \widehat{U}$. Therefore, the states $|\nu\rangle$ are eigenstates of the volume operator \widehat{v} with the eigenvalue ν , and \widehat{U} is a translation operator on these states. The operator \widehat{U} is not weakly continuous in the parameter λ_v , and hence a momentum operator does not exist. This introduces a fundamental discreteness in the theory with the scale set by λ_v . A momentum operator can be defined indirectly however, by making use of the expansion of the classical variable $\exp(i\lambda_v p_v)$ as follows,

$$\widehat{p_v} \equiv \frac{1}{2i\lambda_v} \left(\widehat{U} - \widehat{U}^{\dagger} \right). \tag{22}$$

² See also [48], where a Bianchi-I *like* model is polymer quantized.

From this definition of the momentum operator, the gravitational part of the Hamiltonian becomes (with a symmetric operator ordering),

$$\widehat{H}_v = \frac{3}{16}\widehat{p}_v\widehat{v}\widehat{p}_v - \Lambda\widehat{v}. \tag{23}$$

To study the effective dynamics coming from this Hamiltonian, we compute its expectation value in a suitable 'semi-classical' state (following [37, 38]). The state is defined as,

$$|\psi\rangle = \frac{1}{\mathfrak{N}} \sum_{-\infty}^{+\infty} A_k |\nu_k\rangle,$$

$$A_k = \exp\left(\frac{-(\nu_k - v)^2}{2\sigma_v^2}\right) \exp\left(-ip_v\nu_k\right),$$
(24)

where (v, p_v) are the peaking values for this semi-classical state, σ_v is the gravitational state width, and \mathfrak{N} is a normalization constant.³ The expectation value of the Hamiltonian in this state gives,

$$\langle \widehat{H}_v \rangle = -\frac{3v}{32\lambda_v^2} \left[e^{-\lambda_v^2/\sigma_v^2} \cos(2\lambda_v p_v) - 1 \right] - \Lambda v. \tag{25}$$

With this effective background now available, we turn to the polymer quantization of the anisotropies. The anisotropy momenta operators are defined as,

$$\widehat{p}_{\pm} \equiv \frac{v}{2i\lambda_{+}} \left(\widehat{U}_{\pm} - \widehat{U}_{\pm}^{\dagger} \right), \tag{26}$$

corresponding to the anisotropy degrees of freedom $\boldsymbol{\beta}_{\pm} = v\beta_{\pm}$, and the translation variables $U_{\pm} = \exp{(i\lambda_{\pm}p_{\pm}/v)}$, with the anisotropy polymer scales λ_{\pm} . The expectation value of the anisotropy Hamiltonians (H_{\pm}) is calculated in the Gaussian state,

$$|\psi^{\pm}\rangle = \frac{1}{\Re'} \sum_{-\infty}^{+\infty} A_k^{\pm} |u^{\pm}\rangle,$$

$$A_k^{\pm} = \exp\left(-\frac{(B^{\pm} - B_0^{\pm})^2}{2\sigma_+^2}\right) \exp\left(-ip_{\pm}B^{\pm}\right), \tag{27}$$

where, \mathfrak{R}' is a normalization constant, (B_0^{\pm}, p_{\pm}) , are the peaking values for the anisotropies β_{\pm} and their corresponding conjugate momenta, and σ_{\pm} are the state widths.⁴ The expectation value is computed to be,

$$\langle \hat{H}_{\pm} \rangle = -\frac{v}{96\lambda_{\pm}^2} \left(e^{-\lambda_{\pm}^2/v^2 \sigma_{\pm}^2} \cos\left(\frac{2\lambda_{\pm} p_{\pm}}{v}\right) - 1 \right). \tag{28}$$

³ We choose a polymer lattice with $\nu_k = v + k\lambda_v$.

⁴ Again, we choose a polymer lattice with $B^{\pm} = B_0^{\pm} + k\lambda_{\pm}$.

The total polymer quantized effective gravitational Hamiltonian becomes,

$$H_{g} = -\frac{3v}{32\lambda_{v}^{2}} \left(e^{-\lambda_{v}^{2}/\sigma_{v}^{2}} \cos(2\lambda_{v}p_{v}) - 1 \right) - \Lambda v - \frac{v}{96} \left(\frac{1}{\lambda_{+}^{2}} + \frac{1}{\lambda_{-}^{2}} \right) + \frac{v}{96} \left(\frac{1}{\lambda_{+}^{2}} e^{-\lambda_{+}^{2}/v^{2}\sigma_{+}^{2}} \cos\left(\frac{2\lambda_{+}p_{+}}{v}\right) + \frac{1}{\lambda_{-}^{2}} e^{-\lambda_{-}^{2}/v^{2}\sigma_{-}^{2}} \cos\left(\frac{2\lambda_{-}p_{-}}{v}\right) \right).$$
 (29)

B. Polymer quantized scalar field on a polymer Bianchi-I background

We now couple a polymer quantized massless scalar field to the effective gravitational background given by the Hamiltonian (29). The fundamental matter variables are chosen to be,

$$\Phi = v\phi , \ U_{\phi} = \exp\left(\frac{i\lambda_{\phi}p_{\phi}}{v}\right),$$
(30)

where λ_{ϕ} is the matter polymer scale parameter, and the variable v represents the peaking value of the volume which is necessary to provide the appropriate density weight [17]. The basis states are represented by $|\mu\rangle$ with the orthogonality relation,

$$\langle \mu | \mu' \rangle = \delta_{\mu,\mu'},$$
 (31)

and operator action,

$$\widehat{\Phi}|\mu\rangle = \mu|\mu\rangle , \ \widehat{U}_{\phi}|\mu\rangle = |\mu + \lambda_{\phi}\rangle.$$
 (32)

Once again, the momentum operator \hat{p}_{ϕ} has to be defined indirectly as,

$$\widehat{p_{\phi}} \equiv \frac{v}{2i\lambda_{\phi}} \left(\widehat{U}_{\phi} - \widehat{U}_{\phi}^{\dagger} \right). \tag{33}$$

We now compute the expectation value of the scalar field Hamiltonian $(p_{\phi}^2/2v)$ in a semi-classical Gaussian state taken to be,

$$|\chi\rangle = \frac{1}{\widetilde{\mathfrak{N}}} \sum_{-\infty}^{+\infty} C_k |\mu_k\rangle,$$

$$C_k = \exp\left(\frac{-(\phi_k - \phi)^2}{2\sigma_\phi^2}\right) \exp\left(-ip_\phi\phi_k\right),$$
(34)

where, (ϕ, p_{ϕ}) are the peaking values for the scalar field and its conjugate momentum, σ_{ϕ} is the state width, and $\widetilde{\mathfrak{N}}$ is a normalization factor.⁵ The expectation value is computed to be,

$$\langle \widehat{H}_{\phi} \rangle = -\frac{v}{4\lambda_{\phi}^{2}} \left(e^{-\lambda_{\phi}^{2}/v^{2}\sigma_{\phi}^{2}} \cos\left(\frac{2\lambda_{\phi}p_{\phi}}{v}\right) - 1 \right). \tag{35}$$

 $^{^{5}}$ Here $\phi_{k}=\mu_{k}/v,$ and we choose a lattice with $\phi_{k}=\phi+k\lambda_{\phi}.$

The total physical Hamiltonian (17) is the sum of the gravitational (29) and the matter (35) Hamiltonians,

$$H_{p} = -\frac{3v}{32\lambda_{v}^{2}}e^{-\lambda_{v}^{2}/\sigma_{v}^{2}}\cos(2\lambda_{v}p_{v}) - v\left(\Lambda - \frac{3}{32\lambda_{v}^{2}} + \frac{1}{96\lambda_{+}^{2}} + \frac{1}{96\lambda_{-}^{2}} + \frac{1}{4\lambda_{\phi}^{2}}\right) + \frac{v}{96}\left[\frac{1}{\lambda_{+}^{2}}e^{-\lambda_{+}^{2}/v^{2}\sigma_{+}^{2}}\cos\left(\frac{2\lambda_{+}p_{+}}{v}\right) + \frac{1}{\lambda_{-}^{2}}e^{-\lambda_{-}^{2}/v^{2}\sigma_{-}^{2}}\cos\left(\frac{2\lambda_{-}p_{-}}{v}\right)\right] + \frac{v}{4\lambda_{\phi}^{2}}e^{-\lambda_{\phi}^{2}/v^{2}\sigma_{\phi}^{2}}\cos\left(\frac{2\lambda_{\phi}p_{\phi}}{v}\right).$$
(36)

III. EFFECTIVE FRIEDMANN EQUATION

Before proceeding to discuss the effective dynamics generated by the physical Hamiltonian above, we reformulate this model into an effective Friedmann equation. Note that our main emphasis in the rest of the article will not be on this equation for two primary reasons: (i) We are working in a fixed time gauge, and have (strongly) solved the Hamiltonian constraint at the classical level. Therefore the constraint does not exist anymore; and (ii) When writing the Friedmann equation, matter contributions (and in particular various matter parameters) appear obscured by referring only to the energy densities, whereas we want to explicitly refer to, and discuss the effects of, the matter polymer scale λ_{ϕ} on the dynamics.

Nevertheless, since most of the literature does discuss the effective Friedmann equation, we provide this description here. To begin with, we first derive the Friedmann equation for the classical Bianchi-I model in the Misner variables we consider here. This will help clarify the process, and set the stage for deriving it in the polymer case.

To begin, we have to rewrite the Hamiltonian constraint $(\mathcal{H} = -H_P + P_T \approx 0)$ as the Friedmann equation (in terms of the mean Hubble parameter H_b , and the matter energy densities). The mean Hubble parameter is $H_b = \dot{v}/3v$, the energy density corresponding to the cosmological constant is $\rho_{\Lambda} = \Lambda$, the energy density of the dust field is $\rho_D = P_T/v$ (since P_T is the dust Hamiltonian density), and the scalar field energy density is $\rho_{\phi} = H_{\phi}/v$ where H_{ϕ} is given in (18). Since the anisotropies β_{\pm} act as scalar fields, we can define an equivalent energy density for them as, $\rho_{\pm} \equiv H_{\pm}/v$ (with H_{\pm} in (18)). This gives the total 'matter' energy density (including contributions from the anisotropies and the cosmological constant) as, $\rho_{\text{tot}} = \rho_+ + \rho_- + \rho_\phi + \rho_D + \rho_\Lambda$.

Solving the Hamiltonian constraint for the mean Hubble parameter (after substituting \dot{v} in terms

of p_v from its equation of motion) then gives,

$$H_b^2 = \frac{1}{12}\rho_{\text{tot}}.$$
 (37)

We can also compute how the shear scalar is related to the anisotropy energy densities, and find that,

$$\Sigma^2 = \frac{1}{6}(\rho_+ + \rho_-). \tag{38}$$

In terms of this shear scalar, the Friedmann equation can be recast into a more standard form,

$$H_b^2 = \frac{1}{12}\rho_{\text{tot}} = \frac{1}{12}\left(\rho_+ + \rho_- + \rho_\phi + \rho_D + \rho_\Lambda\right) = \frac{1}{12}\left(\rho_+ + \rho_- + \rho_M\right) = \frac{1}{12}\rho_M + \frac{1}{2}\Sigma^2,\tag{39}$$

where we have defined ρ_M as the sum of all matter contributions.

We now repeat the same steps for the polymer case, with the difference being that, the scalar field energy density is given by $\langle \hat{\rho}_{\phi} \rangle = \langle \hat{H}_{\phi} \rangle / v$ (with $\langle \hat{H}_{\phi} \rangle$ given in (35)), and the effective anisotropy energy densities are given as $\langle \hat{\rho}_{\pm} \rangle = \langle \hat{H}_{\pm} \rangle / v$ (with $\langle \hat{H}_{\pm} \rangle$ given in (28)). This gives the total 'matter' energy density as, $\rho_{\text{tot}} = \langle \hat{\rho}_{+} \rangle + \langle \hat{\rho}_{-} \rangle + \langle \hat{\rho}_{\phi} \rangle + \rho_{D} + \rho_{\Lambda}$. Solving the Hamiltonian constraint then gives us the effective Friedmann equation,

$$H_b^2 = \frac{\rho_{\text{tot}}}{12} \left(1 - \frac{\rho_{\text{tot}}}{\tilde{\rho}} \right) + f(\lambda_v, \sigma_v), \tag{40}$$

where,

$$f(\lambda_v, \sigma_v) \equiv \frac{e^{-2\lambda_v^2/\sigma_v^2} - 1}{16^2 \lambda_v^2} \tag{41}$$

is a function that encodes the effects of a finite polymer scale and a finite state width, 6 and,

$$\tilde{\rho} = \frac{3}{16\lambda_n^2} \tag{42}$$

is the critical energy density. We note that while there is no effective Friedmann equation for loop quantized Bianchi-I models [49, 50], one can be derived for the polymer quantization scheme presented here, and our results are comparable to those found in [8] (we recently became aware of [51], where the authors carry out a quantization of Bianchi-I (and Bianchi-II) with a deformed

⁶ Note that $f \to 0$ in the limit that the semi-classical state is sharply peaked $\sigma_v \to \infty$ (independently of the polymer scale λ_v). In the limit that the polymer scale vanishes $\lambda_v \to 0$ (which corresponds to standard quantization), but the state width σ_v remains finite, $f \sim \mathcal{O}(1/\sigma_v^2)$.

commutation relation, and also report a similar effective Friedmann equation. See also [52] for a comparison of the two approaches).

We can also compute the relation between the shear scalar and the effective anisotropy energy densities,

$$\Sigma^{2} = \frac{\langle \widehat{\rho}_{+} \rangle}{6} \left(1 - \frac{\langle \widehat{\rho}_{+} \rangle}{\widetilde{\rho}_{+}} \right) + \frac{\langle \widehat{\rho}_{-} \rangle}{6} \left(1 - \frac{\langle \widehat{\rho}_{-} \rangle}{\widetilde{\rho}_{-}} \right) + f_{+}(\lambda_{+}, \sigma_{+}, v) + f_{-}(\lambda_{-}, \sigma_{-}, v),$$

$$(43)$$

with,⁷

$$f_{\pm} \equiv \frac{e^{-2\lambda_{\pm}^2/v^2\sigma_{\pm}^2} - 1}{48^2\lambda_{+}^2},\tag{44}$$

and,

$$\tilde{\rho}_{\pm} = \frac{1}{48\lambda_{+}^{2}}.\tag{45}$$

IV. EFFECTIVE DYNAMICS

We now turn to describing the dynamics generated (in dust time) by the effective physical Hamiltonian (36), which contains the effects of polymer quantization in both the gravitational and the matter sectors. The equations of motion are (where an overdot represents differentiation with

⁷ Once again, $f_{\pm} \to 0$ as $\sigma_{\pm} \to \infty$ (independently of the polymer scales λ_{\pm}). In the limit that the polymer scales vanish $\lambda_{\pm} \to 0$ but the state widths σ_{\pm} remain finite, $f_{\pm} \sim \mathcal{O}(1/v^2\sigma_{\pm}^2)$.

respect to dust time),

$$\dot{v} = \frac{3v}{16\lambda_{v}} e^{-\lambda_{v}^{2}/\sigma_{v}^{2}} \sin(2\lambda_{v}p_{v}),
\dot{\beta}_{\pm} = -\frac{1}{48\lambda_{\pm}} e^{-\lambda_{\pm}^{2}/v^{2}\sigma_{\pm}^{2}} \sin\left(\frac{2\lambda_{\pm}p_{\pm}}{v}\right), \quad \dot{p}_{\pm} = 0,
\dot{\phi} = -\frac{1}{2\lambda_{\phi}} e^{-\lambda_{\phi}^{2}/v^{2}\sigma_{\phi}^{2}} \sin\left(\frac{2\lambda_{\phi}p_{\phi}}{v}\right), \quad \dot{p}_{\phi} = 0,
\dot{p}_{v} = \frac{3}{32\lambda_{v}^{2}} e^{-\lambda_{v}^{2}/\sigma_{v}^{2}} \cos(2\lambda_{v}p_{v}) + \frac{1}{96} \left(\frac{1}{\lambda_{+}^{2}} + \frac{1}{\lambda_{-}^{2}}\right) - \frac{3}{32\lambda_{v}^{2}} + \frac{1}{4\lambda_{\phi}^{2}} + \Lambda
- e^{-\lambda_{+}^{2}/v^{2}\sigma_{+}^{2}} \left[\cos\left(\frac{2\lambda_{+}p_{+}}{v}\right) \left(\frac{1}{48v^{2}\sigma_{+}^{2}} + \frac{1}{96\lambda_{+}^{2}}\right) + \sin\left(\frac{2\lambda_{+}p_{+}}{v}\right) \left(\frac{p_{+}}{48v\lambda_{+}}\right)\right]
- e^{-\lambda_{-}^{2}/v^{2}\sigma_{\phi}^{2}} \left[\cos\left(\frac{2\lambda_{-}p_{-}}{v}\right) \left(\frac{1}{48v^{2}\sigma_{-}^{2}} + \frac{1}{96\lambda_{-}^{2}}\right) + \sin\left(\frac{2\lambda_{-}p_{-}}{v}\right) \left(\frac{p_{-}}{48v\lambda_{-}}\right)\right]
- e^{-\lambda_{\phi}^{2}/v^{2}\sigma_{\phi}^{2}} \left[\cos\left(\frac{2\lambda_{\phi}p_{\phi}}{v}\right) \left(\frac{1}{2v^{2}\sigma_{\phi}^{2}} + \frac{1}{4\lambda_{\phi}^{2}}\right) + \sin\left(\frac{2\lambda_{\phi}p_{\phi}}{v}\right) \left(\frac{p_{\phi}}{2v\lambda_{\phi}}\right)\right], \tag{46}$$

and, the mean Hubble parameter H_b is given as,

$$H_b = \frac{\dot{v}}{3v} = \frac{1}{16\lambda_v} e^{-\lambda_v^2/\sigma_v^2} \sin(2\lambda_v p_v). \tag{47}$$

We perform numerical evolutions for various sets of initial conditions $(\alpha, p_{\alpha}, \beta_{+}, p_{+}, \beta_{-}, p_{-}, \phi, p_{\phi})|_{t=0}$, and for different parameter choices $(\lambda_{v}, \lambda_{+}, \lambda_{-}, \lambda_{\phi}, \sigma_{\alpha}, \sigma_{+}, \sigma_{-}, \sigma_{\phi})$. The initial data are selected so that the physical Hamiltonian (36) is strictly non-negative. Moreover, because the physical Hamiltonian in dust time (36) is a constant of motion (time-independent), the dust energy density remains non-negative throughout the entire evolution. Let us first note some salient features of the above equations of motion:

- (i) In the Bianchi-I model, since there is no potential term, the momenta conjugate to the anisotropies (p_+, p_-) are constants of motion. Similarly, since we are considering only a massless scalar field, the scalar field momentum p_{ϕ} is also a constant of motion.
- (ii) The parameters σ_{α} , σ_{+} , σ_{-} , σ_{ϕ} represent corrections due to finite width of the gravitational and matter Gaussian states. These corrections go to zero in the limit that the states are sharply peaked [37, 38].

- (iii) Polymer quantization effects are determined by the parameters $(\lambda_v, \lambda_+, \lambda_-, \lambda_\phi)$. The limit $\lambda_\phi \to 0$ corresponds to a standard scalar field living on a polymer quantized Bianchi-I background, and the simultaneous limits $\lambda_v, \lambda_\pm \to 0$ reproduce a polymer quantized scalar field living on a classical Bianchi-I background.⁸
- (iv) The last terms in the first line of the Hamiltonian (36) show that all of the different polymer scales contribute to the total cosmological constant term. The two anisotropy polymer scales and the scalar field polymer scale contribute positively to Λ , while the volume polymer scale gives a negative contribution. This means that there can be a situation where the overall effective cosmological constant becomes negative, and therefore produces an oscillating universe with multiple bounces and re-collapses. Since we want to focus on the purely quantum effects, we have included a standard Λ term, and given the values of the other polymer scales for various simulations, we choose a value for Λ that does not lead to the overall term being negative.

A. Effective Dynamics Of Bianchi-1 in dust time

We first turn to describing the effective polymer dynamics of the gravitational sector, and then in the later subsection, will look at the effective dynamics with the scalar field included.

Figure 1 shows the results of a typical simulation, and Figure 2 shows the effects of changing various parameters and initial conditions. The initial conditions for both of these figures were chosen to be $(v, P_v)|_{t=0} = (5, 1)$, and $(\beta_{\pm}, p_{\pm}) = (2, 1)$, and the parameter values were taken to be $(\lambda_v, \lambda_+, \lambda_-) = (1, 1, 1)$, $\Lambda = 0.1$, and $(\sigma_{\alpha}, \sigma_+, \sigma_-) = (1, 1, 1)$ (in Figure 2, where various parameters and initial conditions are varied, the captions indicate which variable was changed).

Figure 1 shows that when all anisotropy parameters are set equal with identical initial conditions for the corresponding variables, both anisotropies have the same evolution. The dynamics of the volume variable indicates a bouncing universe with expansion taking place before and after the bounce (as observed in [24] for an FLRW universe). In Figure 2, we illustrate how the evolution of anisotropies with respect to dust time changes when varying the polymer scales, state widths,

⁸ Given that we are taking three different polymer scales for the gravitational variables, we could also consider 'strange' limits where one of them vanishes but the others do not. For example, we could take $\lambda_v \to 0$ while simultaneously keeping λ_{\pm} fixed at some non-zero value. This would represent a scenario where the volume variable behaves classically, while the anisotropies exhibit polymer quantization effects. While an interesting mathematical curiosity, such limits do not seem physically reasonable 13

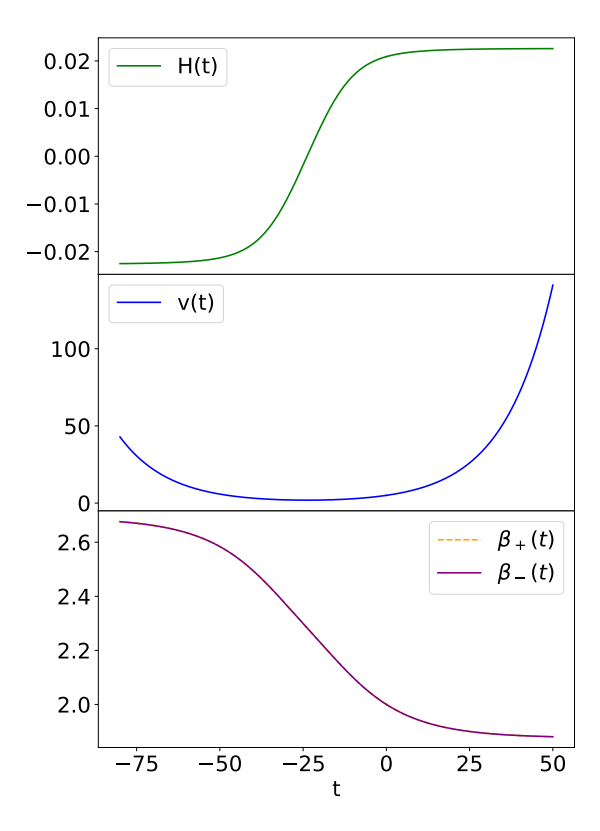


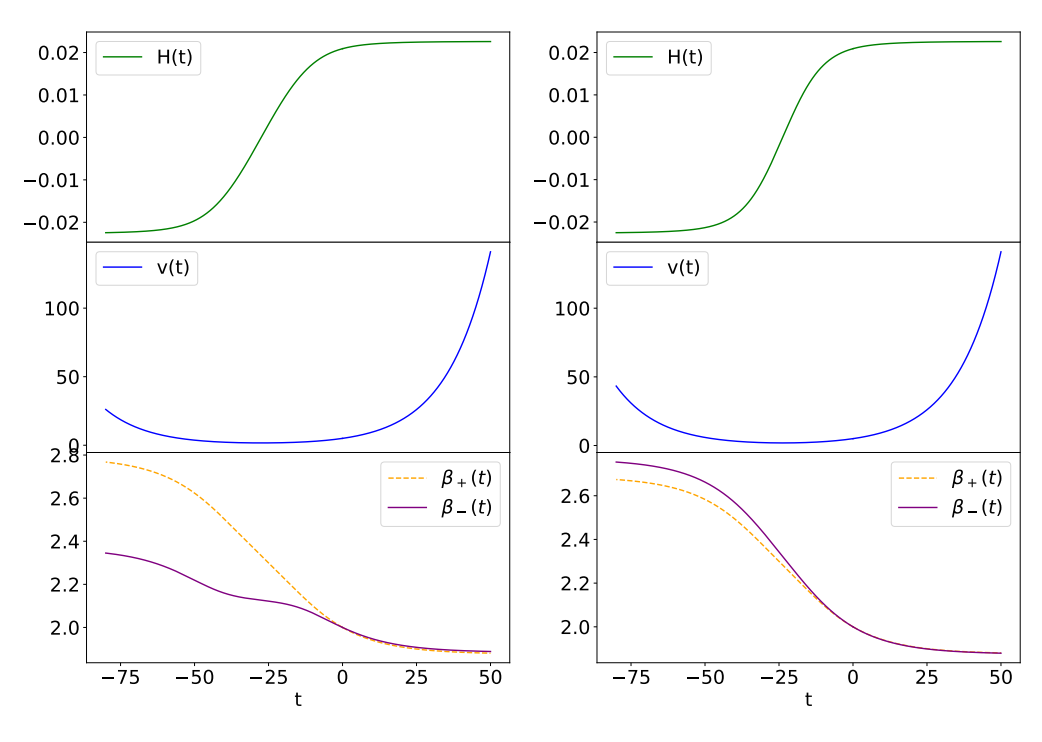
FIG. 1: Results of a typical simulation showing the (dust) time evolution of the Hubble parameter, volume and anisotropies. Both anisotropies show same dynamics since the initial conditions are kept the same.

and initial data. This change in parameters also affects the evolution of the volume variable, and in particular, there is a change in the location of the quantum bounce.

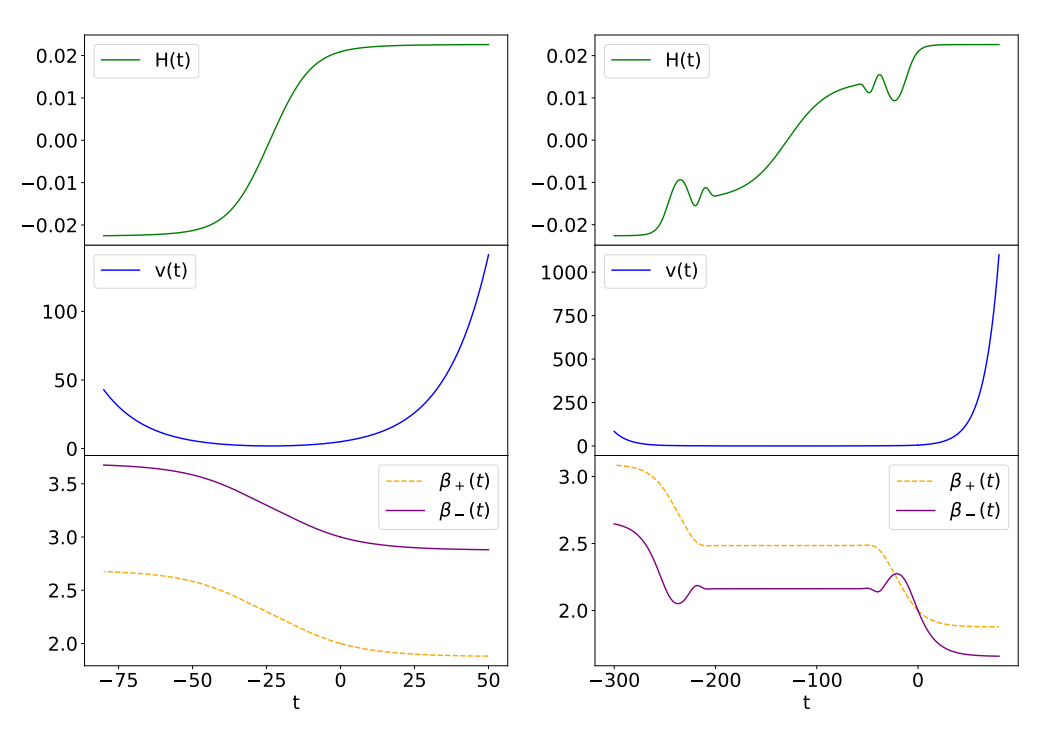
B. Polymer Bianchi-I with a polymer scalar field

We now consider the full system of differential equations (46), which govern polymer Bianchi-I coupled to a polymer scalar field, and solve them numerically to analyze the resulting dynamics.

Figure 3 shows a typical evolution, and the effect of varying the anisotropy parameters. For all the remaining Figures (3 - 13), initial conditions were chosen to be $(v, p_v)|_{t=0} = (15, 1)$, $(\beta_{\pm}, p_{\pm})|_{t=0} = (2, 1)$, and $(\phi, p_{\phi})|_{t=0} = (2, 3)$ with parameter values $(\lambda_v, \lambda_+, \lambda_-, \lambda_{\phi}) = (1, 1, 1, 1)$, $\Lambda = 0.07$ and $(\sigma_v, \sigma_+, \sigma_-, \sigma_{\phi}) = (1, 1, 1, 1)$. If any parameter values differ, or were varied, they are indicated in



- (a) The two anisotropy polymer scales are varied with $\lambda_+=1,$ and $\lambda_-=2.$
- (b) The two anisotropy state widths are varied with $\sigma_{+}=1$, and $\sigma_{-}=2$.



- (c) The anisotropy initial conditions are varied with $(\beta_+, \beta_-)|_{t=0} = (2, 3)$.
- (d) The two anisotropy momenta are varied with $p_{+}=1$, and $p_{-}=3$.

FIG. 2: Evolution of Bianchi-I cosmological quantities with varying parameter values and initial conditions.

the captions.

Figure 4 shows the effects of varying the volume polymer scale λ_v , while keeping the matter and the anisotropy polymer scales fixed at $\lambda_{\pm} = \lambda_{\phi} = 1$. The three distinct cases are $\lambda_v < \lambda_{\pm}$, $\lambda_v = \lambda_{\pm}$, and $\lambda_v > \lambda_{\pm}$, indicating situations where polymerization in the volume variable happens before, at the same scale, and after (respectively) polymerization in the anisotropies (and the scalar field). Given the construction of our model, the first two cases are physically reasonable.

Figure 5 illustrates the effect on the dynamical behavior of the Hubble parameter, volume, anisotropies and the scalar field when the matter polymer scale λ_{ϕ} is varied. We notice that there is a clear difference in the dynamics of the universe (in both volume, and anisotropies), and in particular, the dynamics of the limiting case $\lambda_{\phi} = 10^{-6}$ - which represents Schrodinger quantization of the scalar field - are significantly different from the other cases where the field is polymer quantized. This shows that polymer quantization of the matter sector can have a significant effect on the gravitational observables.

We also note that there is variation in the location of the quantum bounce as the matter polymer scale, and the initial conditions are varied. These are illustrated in Figures 6 and 7 respectively (to describe the effect of changing the initial conditions, we fix different values for the physical Hamiltonian H_p , and solve for p_v).

Lastly, we find that for all the gravitational variables (volume, and the two anisotropies), there is asymmetric evolution across the bounce. As in [24], we quantify this asymmetry by computing the absolute value of the difference between the relevant variable after the bounce, and before the bounce. The results are shown in Figure 8. We find that this asymmetry depends on the choice of the matter polymer scale λ_{ϕ} , and that for the volume variable, it continues to increase as (dust) time goes on, whereas for the anisotropies, it increases at first, but eventually appears to reach a steady state. Figure 9 shows the dynamics of the physical Hamiltonian after subtracting its initial value for a typical solution. Since, in dust time, the physical Hamiltonian H_p is a constant of the motion, its value should remain unchanged under evolution. We find that this is indeed the case, and serves as a good check of our numerics.

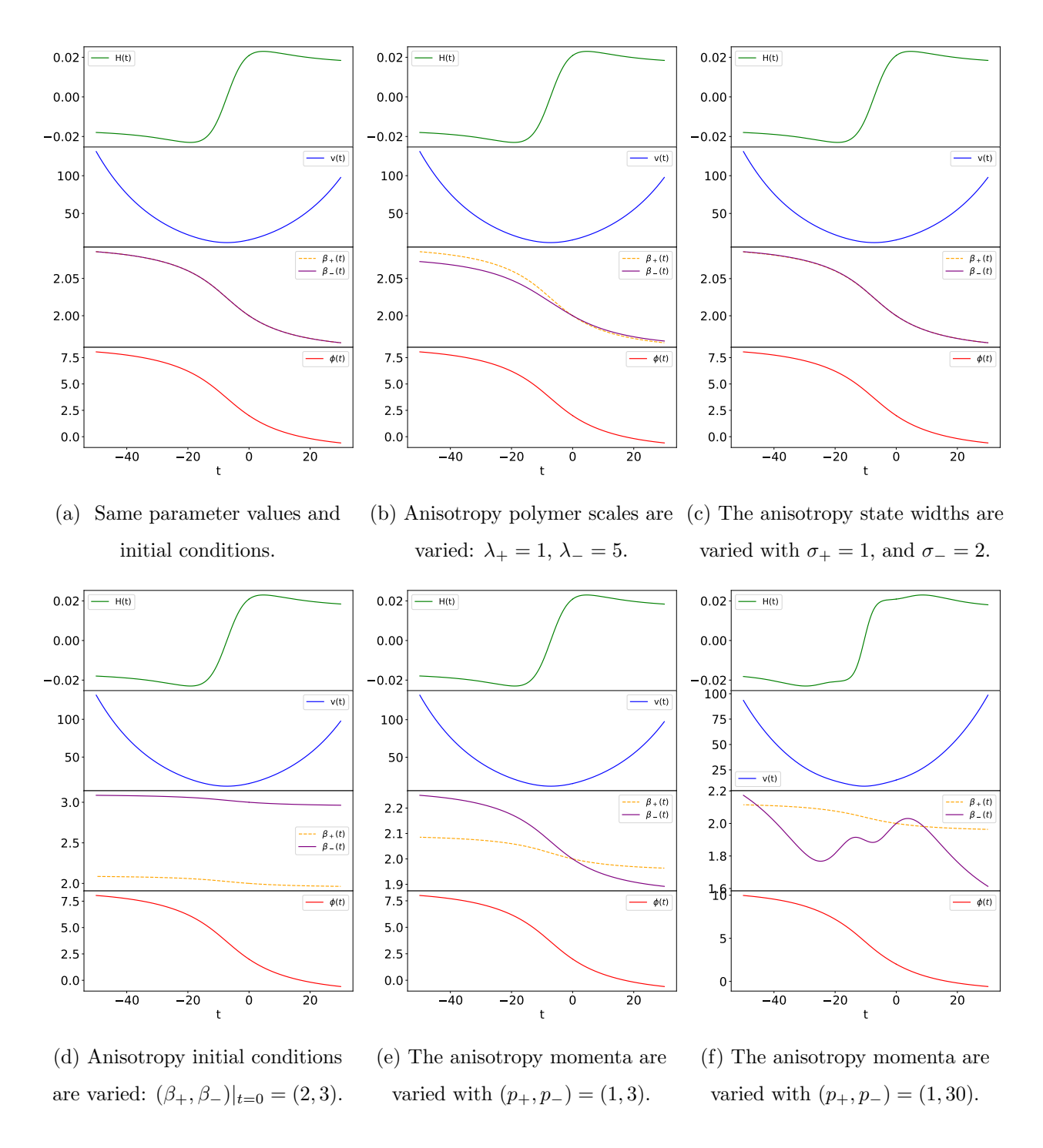


FIG. 3: Time evolution of cosmological quantities in Bianchi-I with varying parameter values and initial conditions.

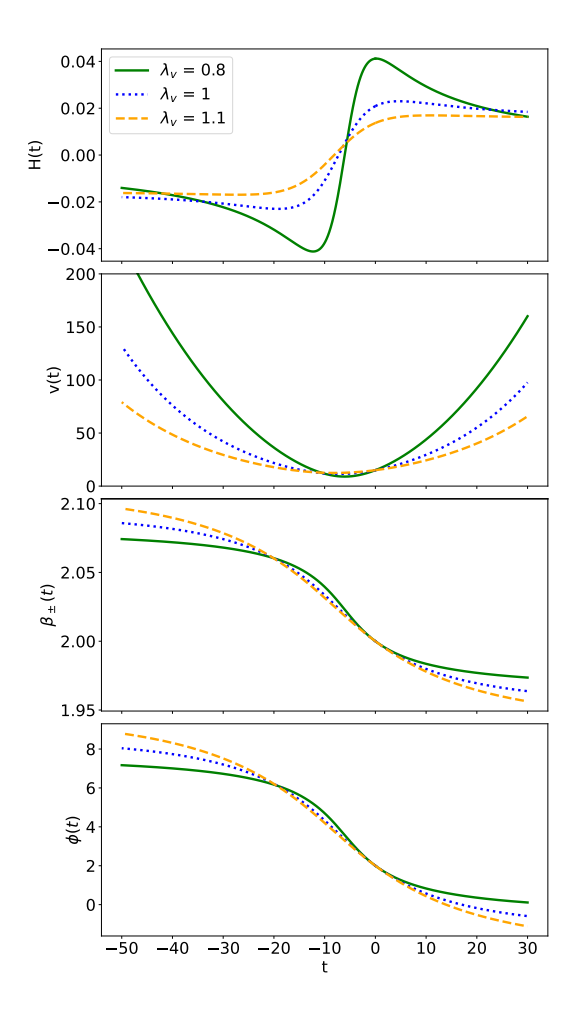


FIG. 4: The effects of varying the volume polymer scale λ_v on the evolution of various cosmological quantities and the scalar field. The differences are clearly visible.

C. Directional scale factors, Hubble parameters, and shears

We have been looking at the dynamical trajectories of the Misner variables. However, once we have solved the equations of motion (46), it is straightforward to compute the trajectories of the usual scale factors given in (9). Similarly, we can compute the directional (and mean) Hubble parameters (5, 6) as well as the directional (and mean) shears (7, 8). All of these quantities (along with their means), for a typical solution, are shown in Figure 10.

The effects of varying the matter polymer scale λ_{ϕ} on the dynamics of the scale factors (and their mean), the Hubble parameters (and their mean), and the shear scalars (and their mean) are

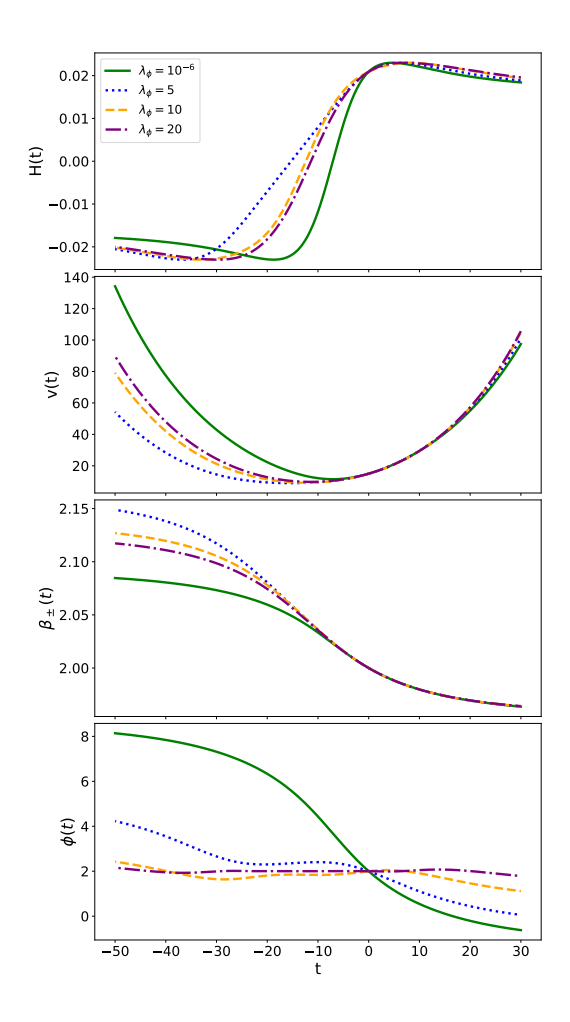


FIG. 5: The effects of varying the matter polymer scale λ_{ϕ} on the evolution of various cosmological quantities and the scalar field. The differences are clearly visible. The green (solid) curve shows the Schrödinger limit.

shown in Figures 11, 12, and 13 respectively.

V. SUMMARY

We have presented here a model of polymer quantization of a homogeneous but anisotropic Bianchi-I universe coupled to a polymer quantized massless scalar field. We use a pressureless dust field as an internal clock, and study the resultant effective dynamics obtained by taking the expectation value of the Hamiltonian operator in a semi-classical Gaussian state. This presents a

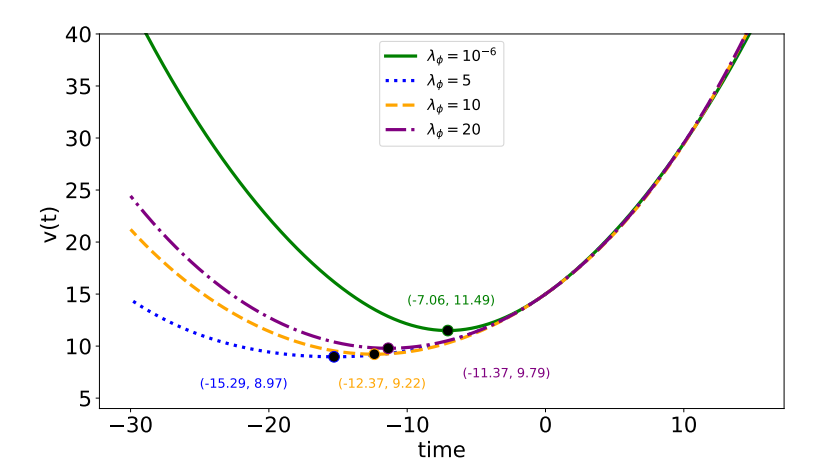


FIG. 6: Dependence of the bounce on the matter polymer scale λ_{ϕ} . The circles show the point of the bounce, and the numerical values indicate the time and the minimum volume at the bounce respectively ($t_{\text{bounce}}, v_{\text{bounce}}$). The green (solid) curve shows the Schrodinger limit.

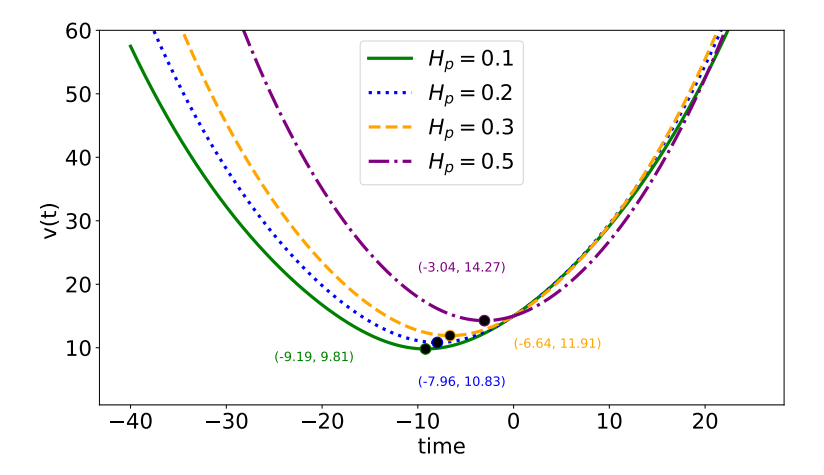


FIG. 7: Variation in the bounce as the value of the total Hamiltonian H_p is varied. The circles show the point of the bounce, and the numerical values indicate the time and the minimum volume at the bounce respectively $(t_{\text{bounce}}, v_{\text{bounce}})$. This shows dependence on initial conditions.

complete (effective) quantization of both the gravity and the matter sectors, extending the results first obtained in the FLRW case [24] to an anisotropic universe.

We found that for a consistent polymer quantization of the anisotropies, we first have to poly-

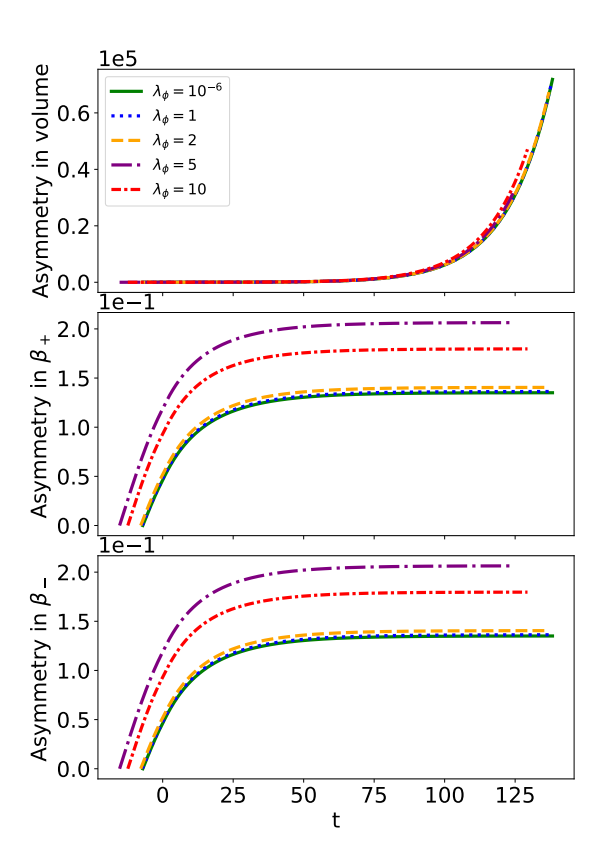


FIG. 8: Asymmetry in the volume and anisotropies across the bounce as the matter polymer scale λ_{ϕ} is varied. The green (solid) curve shows the Schrodinger limit.

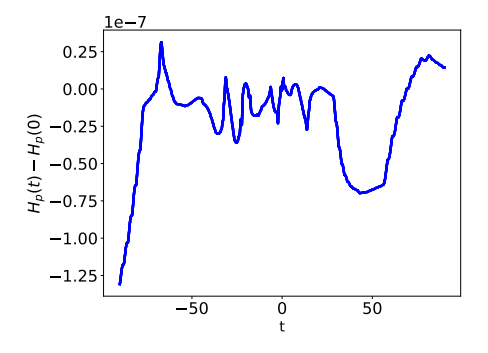


FIG. 9: Time variation of the physical Hamiltonian for a typical solution. The small scale of variations indicates good control over numerics.

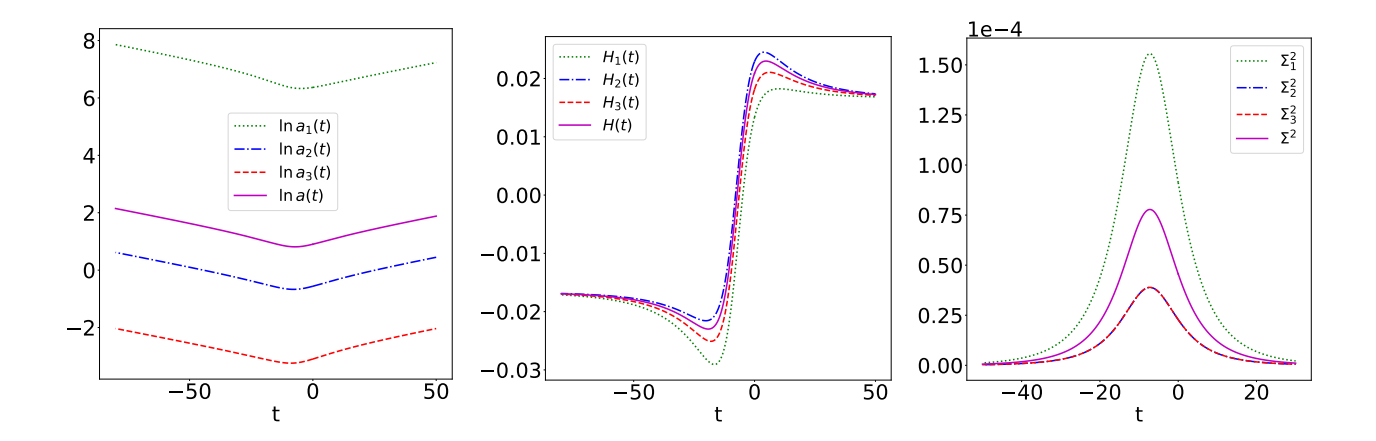


FIG. 10: The three directional scale factors, Hubble parameters, shears, and their corresponding means.

merize the volume variable, compute an effective (volume) background, and then polymerize the anisotropies on that background (similar to what is done for the scalar field). This is because, in the Misner variables considered here, the anisotropy momenta are densities and not scalars. Whereas, to perform a polymer quantization, we have to consider variables constructed by exponentiating the momenta which requires them to be scalars. An alternate possibility would be to transform these momenta to scalars, however, as it turns out, such a transformation is non-canonical and produces a complicated Hamiltonian. We leave the quantization of that Hamiltonian to future studies.

Our main results indicate that having different polymer scales, or state widths, for the two anisotropy variables gives rise to distinct cosmological dynamics. Similarly, depending on whether the volume polymer scale is larger than, equal to, or smaller than the anisotropy scale, the resultant dynamics are qualitatively different. Furthermore, the location of the bounce depends on initial conditions, and there is asymmetric evolution across the bounce for both the volume, and the anisotropies. We also derived an effective Friedmann equation (which is not known yet for LQC models) that shows a quantum bounce, and we computed a relationship between the shear scalar and the effective anisotropy energy densities, similar in form to the effective Friedmann equation.

One of the main objectives of this study was to elucidate the effect of the matter polymer scale on the dynamics of the universe. We found that polymer quantization of the scalar field produces substantially different dynamics than a standard Schrodinger quantized, or classical, scalar field.

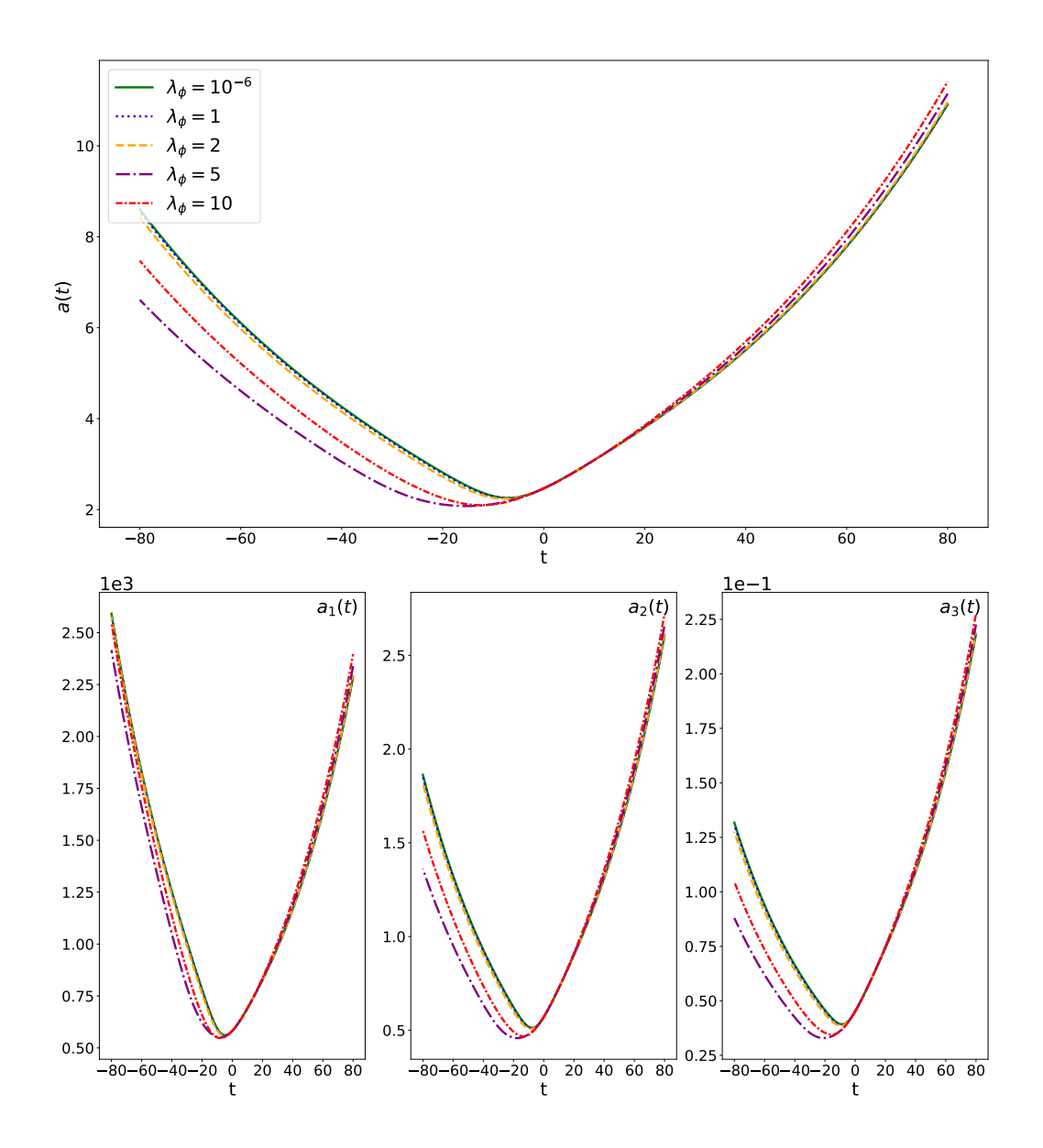


FIG. 11: Variation in the three directional scale factors and their mean as λ_{ϕ} is varied. The green (solid) curves show the Schrodinger limit.

Furthermore, we saw that varying the matter polymer scale leads to qualitatively different behavior for the volume and the anisotropies, as well as other cosmological quantities like the scale factors, the Hubble parameters, and the shear scalars. Furthermore, the matter polymer scale also affects the location of the bounce, as well as the amount of asymmetry in the volume and anisotropies (before and after the bounce).

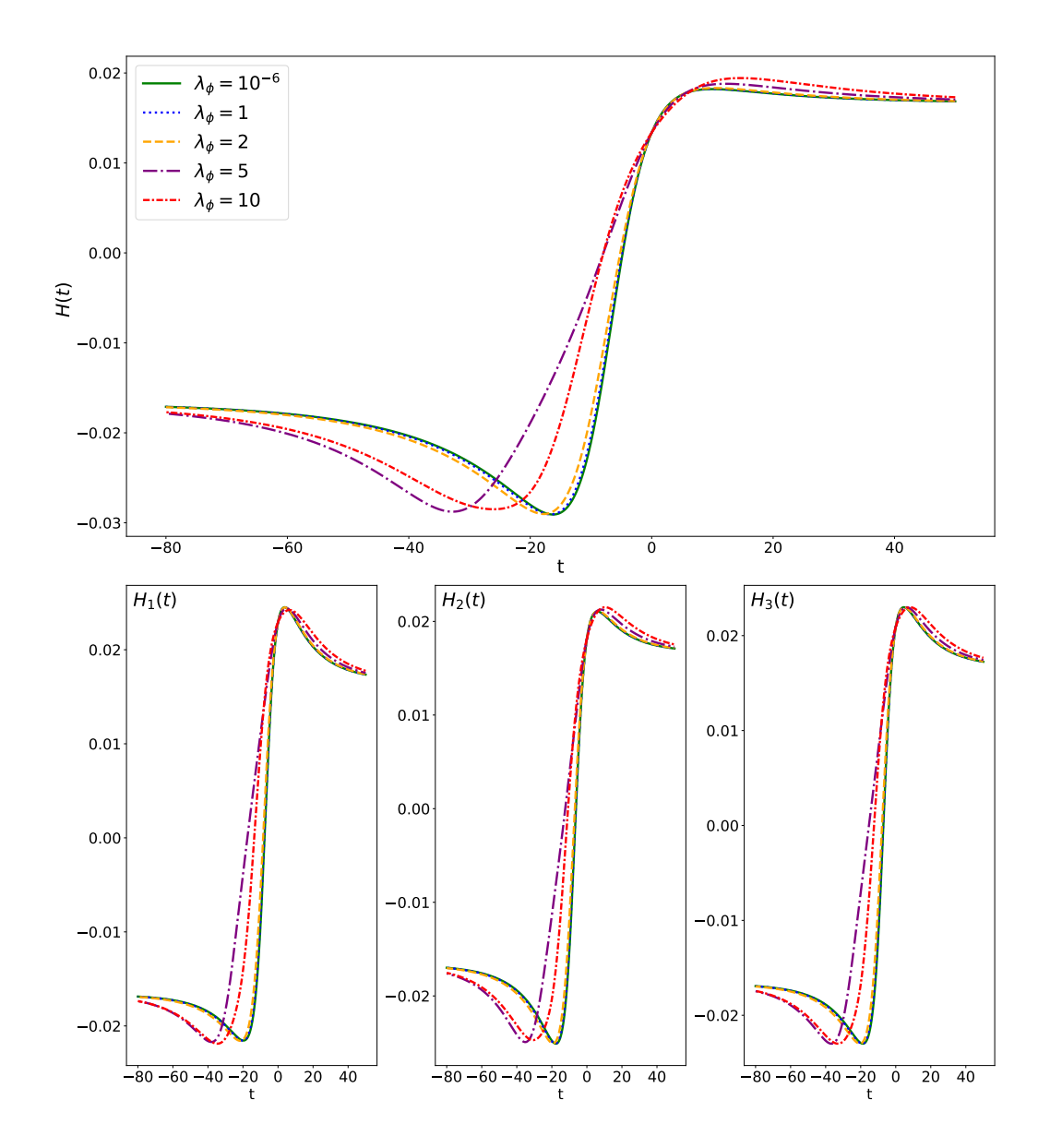


FIG. 12: Variation in the three directional Hubble parameters and their mean as λ_{ϕ} is varied. The green (solid) curves show the Schrodinger limit.

A useful extension of this work would be to the Bianchi-IX (Mixmaster) model [53] where, as the singularity is approached, the geometry is approximated well by a Bianchi-I solution with (Kasner [54]) transitions taking place between different Bianchi-I solutions [55]. A study of the semiclassical dynamics of this model (where only the gravity part is polymer quantized) appears in [56], and an analysis of the Mixmaster dynamics in the dust time gauge was discussed in [45].

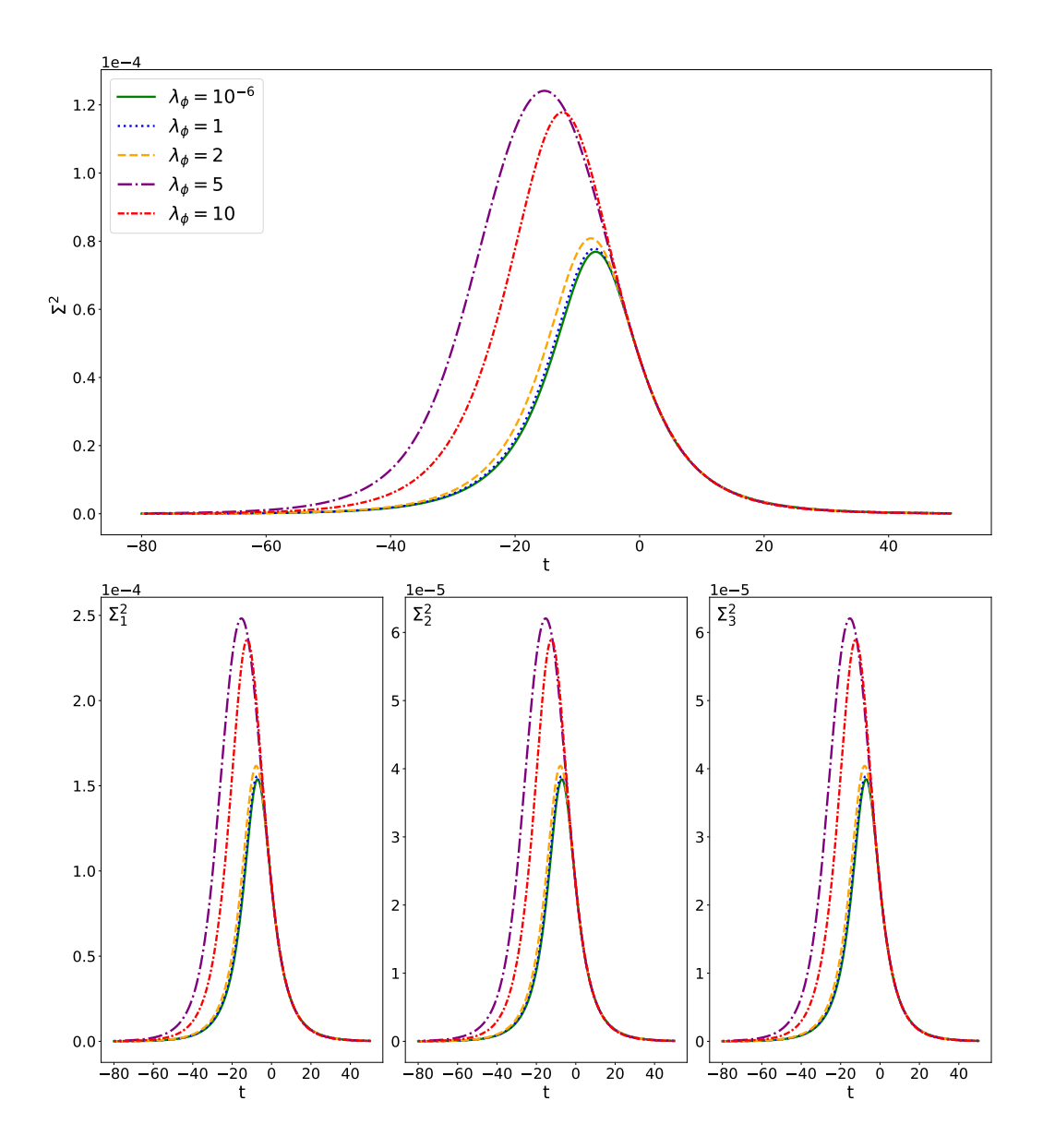


FIG. 13: Variation in the three directional shears and their mean as λ_{ϕ} is varied. The green (solid) curves show the Schrodinger limit.

It will be interesting to see how the polymer quantization presented here (and in particular the polymerized matter field) will affect the Kasner transitions, and what its implications will be for the Belinski-Khalitnikov-Lifshitz (BKL) conjecture [57]. We leave this for future studies.

Overall, this project is a further step in the direction of analyzing the polymer quantized dynamics of gravity with matter where both of these sectors are treated on an equal footing (see also

[58–60] for approaches where both sectors are quantized simultaneously). While we were limited here to discussing the effective dynamics that arise from this approach, and also with regards to the particular choice of polymer quantization we made, this study serves as a prelude towards a complete (polymer) quantum treatment of gravity with matter in general, and Bianchi-I cosmology with a scalar field in particular.

ACKNOWLEDGMENTS

SMH would like to thank Dr. Rizwan Khalid for helpful discussions and suggestions. This project was supported by the Higher Education Commission (HEC) of Pakistan through NRPU grant No. 20-15435.

^[1] I. Agullo and P. Singh, "Loop quantum cosmology." in *Loop Quantum Gravity: The First 30 Years*, edited by A. Ashtekar and J. Pullin (WSP, 2017) pp. 183–240, arXiv:1612.01236 [gr-qc].

^[2] A. Ashtekar and P. Singh, Class. Quant. Grav. 28, 213001 (2011), arXiv:1108.0893 [gr-qc].

^[3] B.-F. Li, P. Singh, and A. Wang, Phys. Rev. D 97, 084029 (2018), arXiv:1801.07313 [gr-qc].

^[4] H. Halvorson, Studies in History and Philosophy of Science Part B: Studies in History and Philosophy of Modern Physics **35**, 45–56 (2004).

^[5] A. Ashtekar, S. Fairhurst, and J. L. Willis, Class. Quant. Grav. 20, 1031 (2003), arXiv:gr-qc/0207106.

^[6] J. Ben Achour and E. R. Livine, Phys. Rev. D 99, 126013 (2019), arXiv:1806.09290 [gr-qc].

^[7] G. Montani, C. Mantero, F. Bombacigno, F. Cianfrani, and G. Barca, Phys. Rev. D 99, 063534 (2019), arXiv:1806.10364 [gr-qc].

^[8] E. Giovannetti, G. Montani, and S. Schiattarella, Phys. Rev. D 105, 064011 (2022), arXiv:2105.00360[gr-qc].

^[9] E. Giovannetti and G. Montani, Phys. Rev. D 100, 104058 (2019), arXiv:1907.12083 [gr-qc].

^[10] G. Barca, P. Di Antonio, G. Montani, and A. Patti, Phys. Rev. D 99, 123509 (2019), arXiv:1902.02128 [gr-qc].

^[11] E. Giovannetti, G. Barca, F. Mandini, and G. Montani, Universe 8, 302 (2022), arXiv:2006.10614 [gr-qc].

^[12] G. Barca, E. Giovannetti, and G. Montani, Universe 7, 327 (2021), arXiv:2109.08645 [gr-qc].

- [13] A. Ashtekar, J. Lewandowski, and H. Sahlmann, Class. Quant. Grav. 20, L11 (2003), arXiv:gr-qc/0211012.
- [14] A. Corichi, T. Vukasinac, and J. A. Zapata, Phys. Rev. D 76, 044016 (2007), arXiv:0704.0007 [gr-qc].
- [15] A. Laddha and M. Varadarajan, Class. Quant. Grav. 27, 175010 (2010), arXiv:1001.3505 [gr-qc].
- [16] A. Kreienbuehl and T. Pawłowski, Phys. Rev. D 88, 043504 (2013), arXiv:1302.6566 [gr-qc].
- [17] G. M. Hossain, V. Husain, and S. S. Seahra, Phys. Rev. D 81, 024005 (2010), arXiv:0906.2798 [astro-ph.CO].
- [18] G. M. Hossain, V. Husain, and S. S. Seahra, Phys. Rev. D 82, 124032 (2010), arXiv:1007.5500 [gr-qc].
- [19] S. M. Hassan, V. Husain, and S. S. Seahra, Phys. Rev. D 91, 065006 (2015), arXiv:1409.6218 [astro-ph.CO].
- [20] S. M. Hassan and V. Husain, Class. Quant. Grav. 34, 084003 (2017), arXiv:1705.00398 [gr-qc].
- [21] M. Ali and S. S. Seahra, Phys. Rev. D **96**, 103524 (2017), arXiv:1709.03960 [gr-qc].
- [22] A. Mujtaba and S. M. Hassan, (2025), arXiv:2508.16416 [gr-qc].
- [23] V. Husain and A. Kreienbuehl, Phys. Rev. D 81, 084043 (2010).
- [24] A. Zulfiqar and S. M. Hassan, JCAP (2025), arXiv:2502.04875 [gr-qc].
- [25] T. Schucker, A. Tilquin, and G. Valent, Mon. Not. Roy. Astron. Soc. 444, 2820 (2014), arXiv:1405.6523 [astro-ph.CO].
- [26] L. Campanelli, P. Cea, and L. Tedesco, Phys. Rev. Lett. 97, 131302 (2006), [Erratum: Phys.Rev.Lett. 97, 209903 (2006)], arXiv:astro-ph/0606266.
- [27] Ö. Akarsu, S. Kumar, S. Sharma, and L. Tedesco, Phys. Rev. D 100, 023532 (2019), arXiv:1905.06949 [astro-ph.CO].
- [28] P. K. Aluri et al., Class. Quant. Grav. 40, 094001 (2023), arXiv:2207.05765 [astro-ph.CO].
- [29] M. P. Hertzberg and A. Loeb, Phys. Rev. D 109, 083538 (2024), arXiv:2401.15782 [astro-ph.CO].
- [30] O. Akarsu, E. Di Valentino, S. Kumar, M. Ozyigit, and S. Sharma, Phys. Dark Univ. 39, 101162 (2023), arXiv:2112.07807 [astro-ph.CO].
- [31] A. Ashtekar and E. Wilson-Ewing, Phys. Rev. D 79, 083535 (2009), arXiv:0903.3397 [gr-qc].
- [32] M. de Cesare and E. Wilson-Ewing, JCAP 12, 039 (2019), arXiv:1910.03616 [gr-qc].
- [33] T. Thiemann, Class. Quant. Grav. 15, 1281 (1998), arXiv:gr-qc/9705019.
- [34] A. Laddha and M. Varadarajan, Phys. Rev. D 78, 044008 (2008), arXiv:0805.0208 [gr-qc].
- [35] M. Domagala, M. Dziendzikowski, and J. Lewandowski, in 3rd Quantum Geometry and Quantum Gravity School (2012) arXiv:1210.0849 [gr-qc].
- [36] I. Agullo, A. Wang, and E. Wilson-Ewing, "Loop quantum cosmology: Relation between theory and observations," in *Handbook of Quantum Gravity* (Springer Nature Singapore, 2023) p. 1–46.
- [37] V. Husain and O. Winkler, Phys. Rev. D 75, 024014 (2007), arXiv:gr-qc/0607097.

- [38] V. Taveras, Phys. Rev. D 78, 064072 (2008), arXiv:0807.3325 [gr-qc].
- [39] C. Rovelli and E. Wilson-Ewing, Phys. Rev. D **90**, 023538 (2014), arXiv:1310.8654 [gr-qc].
- [40] V. Husain and T. Pawlowski, Phys. Rev. Lett. 108, 141301 (2012), arXiv:1108.1145 [gr-qc].
- [41] V. Husain and T. Pawlowski, Class. Quant. Grav. 28, 225014 (2011), arXiv:1108.1147 [gr-qc].
- [42] M. Ali, S. M. Hassan, and V. Husain, Phys. Rev. D 98, 086002 (2018), arXiv:1807.03864 [gr-qc].
- [43] M. Ali, S. Moeez Hassan, and V. Husain, Class. Quant. Grav. 36, 234002 (2019), arXiv:1811.05047 [gr-qc].
- [44] M. Ali, V. Husain, S. Rahmati, and J. Ziprick, Class. Quant. Grav. 33, 105012 (2016), arXiv:1512.07854
 [gr-qc].
- [45] M. Ali and V. Husain, Phys. Rev. D **96**, 044032 (2017), arXiv:1707.07098 [gr-qc].
- [46] V. Husain, J. G. Kelly, R. Santacruz, and E. Wilson-Ewing, Phys. Rev. Lett. 128, 121301 (2022), arXiv:2109.08667 [gr-qc].
- [47] K. Giesel, B.-F. Li, and P. Singh, Phys. Rev. D 104, 023501 (2021), arXiv:2012.14443 [gr-qc].
- [48] A. Zulfiqar and S. M. Hassan, In prep (2025).
- [49] A. M. McNamara, S. Saini, and P. Singh, Phys. Rev. D 107, 026003 (2023), arXiv:2210.07257 [gr-qc].
- [50] M. Motaharfar, P. Singh, and E. Thareja, Phys. Rev. D 109, 086013 (2024), arXiv:2311.08465 [gr-qc].
- [51] G. Barca and S. Gielen, (2025), arXiv:2507.01678 [gr-qc].
- [52] G. Barca, E. Giovannetti, and G. Montani, Int. J. Geom. Meth. Mod. Phys. 19, 2250097 (2022), arXiv:2112.08905 [gr-qc].
- [53] C. W. Misner, Phys. Rev. Lett. **22**, 1071 (1969).
- [54] E. Kasner, American Journal of Mathematics 43, 217 (1921).
- [55] C. W. Misner, Phys. Rev. **186**, 1319 (1969).
- [56] M. Muzammil and V. Husain, Phys. Rev. D 111, 084071 (2025), arXiv:2501.14891 [gr-qc].
- [57] V. A. Belinskii, E. M. Lifshitz, and I. M. Khalatnikov, Soviet Physics Uspekhi 13, 745 (1971).
- [58] A. Ashtekar, W. Kaminski, and J. Lewandowski, Phys. Rev. D 79, 064030 (2009), arXiv:0901.0933
 [gr-qc].
- [59] M. Ali and S. Steinhaus, Phys. Rev. D **106**, 106016 (2022), arXiv:2206.04076 [gr-qc].
- [60] M. Han, H. Liu, D. Qu, F. Vidotto, and C. Zhang, Phys. Rev. D 111, 086012 (2025), arXiv:2402.07984
 [gr-qc].